Hindawi
Advances in Civil Engineering
Volume 2023, Article ID 3829385, 10 pages
https://doi.org/10.1155/2023/3829385

Research Article

Study on Solidification Characteristics of Granular Coal Gangue: Fine Sand Paste-Cemented Filling Materials

Daiqiang Deng[1,2] **Runze Wang**[1] **Guodong Cao**[1] **Yihua Liang**[3] **Jinkuan Fan**[1] **Yunfan Ma**[1] **and Yu Gao**[1]

[1]*College of Civil Engineering, Xiangtan University, Xiangtan 411105, China*
[2]*Institute of Mining Engineering, Guizhou Institute of Technology, Guiyang, Guizhou 550003, China*
[3]*Industrial Development Research Center of Guizhou, Guizhou Institute of Technology, Guiyang, Guizhou 550003, China*

Correspondence should be addressed to Guodong Cao; gdcao@xtu.edu.cn and Yihua Liang; 20150631@git.edu.cn

Received 16 March 2023; Revised 20 July 2023; Accepted 10 August 2023; Published 16 September 2023

Academic Editor: Belén González-Fonteboa

Three groups of filling materials with different mix proportions were prepared. PO42.5 grade cement was selected as the binding material, mechanized granular coal gangue and fine sand were used as the filling aggregate, and then the specimens were curing at room temperature and 95% moisture. Through the uniaxial compression test, the influence of gangue–sand ratio, the mass fraction, and curing age on the mechanical properties of filling materials was analyzed. The microstructure analysis of SEM was conducted to explore the internal mechanism of the strength difference of filling materials. The results show that the gangue–sand ratio dramatically influences the uniaxial compressive strength. The strength increases first and then decreases with the gangue–sand ratio increase. The mass fraction of filling paste is positively correlated with specimen strength. When the sand–cement ratio, gangue–sand ratio, and the mass fraction remain unchanged, the longer the curing age, the greater the uniaxial compressive strength of specimens. The specimens with a sand–cement ratio of 3.5 : 1, a gangue–sand ratio of 5 : 5, and a mass fraction of 86% reach the maximum value of 11.03 MPa at a curing age of 10 days. It can be seen that when the gangue–sand ratio is 5 : 5, the filling material has the best mechanical properties, so it can be recommended as the optimal mix proportion for goaf filling. Thus, it provides a solid technical guarantee for the treatment of mine surface collapse disasters and the utilization of bulk coal gangue resources.

1. Introduction

Some enterprises need to burn coal to provide various power in daily production and require coal combustion to meet production needs [1, 2]. With the gradual improvement of gaining various clean energy technologies in recent years, some industries are gradually reducing the use of coal to obtain better economic and environmental benefits [3, 4]. Wind energy, solar energy, biodiesel, tidal energy, and many other forms of energy use and transformation meet or partially meet the production and living requirements. This avoids burning coal and producing dust, smoke, and other toxic and harmful substances, reduces the burning of coal and many cinders, gangue, and other solid waste. The energy use changes from the previous rough gradually to intensive transformation, conform to the national and social vigorously advocated energy conservation and emission reduction, clean production, and other policies [5–9]. In the long-term use of coal, human beings have formed a mature industrial technology process, which has excellent use efficiency in a series of related industrial chains and creates great economic returns and convenience for production and life. As a highly integrated fossil fuel and chemical raw material composition, coal's high utilization rate will continue to be favored, given its outstanding performance in many industrial sectors [10]. Under the needs of the new energy security strategy, domestic researchers have analyzed the technical ways to reduce solid waste and flue gas emissions and discussed relevant countermeasures by drawing on global research experience and taking into account China's national conditions of energy utilization [11]. With the change in energy use, some regions that have long relied on energy development are also exploring new implementation paths. Combining energy use with energy conservation and emission reduction promotes the economic development of the central and western regions [12].

With the increase in complex mining geological conditions, coal mining faces more frequent ground pressure problems. In the process of coal mine mining, the relevant researchers put forward some specific measures to solve protection problems in coal mine filling, which provide a reference for the use of the filling method [13–15]. For the preparation of filling materials using coal gangue and crushed waste rock as aggregates, researchers have used conventional means or advanced X-ray and CT scanning technology to detect the interaction of various materials inside the filling body and analyzed in detail the factors affecting the compactness of granular materials. This provided experience in improving the material formulation of filling materials [16–18]. In the process of coal mine filling and mining, it is necessary to ensure safe production and protect the underground rock formation. Some researchers have studied the mechanical characteristics of the coal seam roof in detail and detected the displacement law of the top plate. Moreover, for the actual situation of the mining process of the sharply inclined coal seam heaving workings, the displacement of top plate was controlled to avoid the destruction of the underground river water system caused by the damage of rock stratum [19, 20]. Researchers combined coal gangue's physical and chemical properties in the research of coal mine solid waste resource utilization. They carried out the mechanical properties of coal gangue-filled materials under high-temperature conditions to analyze the changes of material stress, strain, and porosity with temperature and then derived the influence law of temperature on material deformation mechanism [21, 22]. In the use of microbial technology to improve the performance of coal gangue-filling materials, researchers conducted a study on microbial-induced calcium carbonate precipitation (MICP) solidification of coal gangue-filling materials. It enhanced the solidification and hardening effect of the filling materials in a friendly and nonpolluting environment, provided a new way for the resource utilization of coal gangue [23]. To make the gangue-filling material have good mechanical and flowability, researchers developed self-consolidating cement tailings paste pouring solidified gangue-filling material for iron ore tailings and coal gangue (CG) mixture material. From the solidification hardening effect, the new gangue-filling material has good field use prospects [24].

The performance study of filling materials with granular coal gangue as coarse aggregate and fine sand as fine aggregate can respond to the call for green and sustainable development of the country. It can realize the resource utilization of coal gangue to reduce the encroachment of coal gangue accumulation on the land. It not only avoids the pollution of the surrounding environment but also saves natural stone resources. The mechanism of granular gangue used as the coarse aggregate can significantly improve the utilization rate of coal gangue. Moreover, it can promote the sustainable development of the building materials preparation industry and make the coal industry move closer to the direction of green development.

Gangue has lower hardness and strength than granite, red sandstone, marble, and other dense rock types. The gangue from the parent rock is more easily broken and usually presents a large piece of flake and block appearance type. The research on coal gangue as a coal mine-filling material has been active in recent years, and some experience and conclusions can also play a good role in the relevant research [25–27]. In terms of the fluidity of the granular material slurry and the mechanical properties of the material, the relevant researchers combined the engineering conditions to carry out the study of the influence of the granular mechanism sand on the mechanical properties of the mortar, which provided a reliable technical basis for material optimization [28]. Compared with the granular mechanism sand, the source and origin of the mechanism granular coal gangue in this study are more extensive for the filling needs of coal mine goaf. Researchers can source materials locally at the mine. What we need to consider at the same time is that coal gangue's physical and chemical properties in different regions have specific differences. Even if the coal gangue is produced in the same location, its physical and chemical properties will also have individual differences. This paper studies the gangue of Wantian Coal Mine in Liupanshui City, Guizhou Province, and analyzes the mechanical properties and laws of mechanical granular gangue-filling materials. For other coal mining enterprises, the relevant filling material performance may change to a certain extent, so in other cases still need to be analyzed [29, 30]. In this paper, mechanism granular gangue and fine sand were used as coarse and fine aggregates, respectively. The influence of material dosage on the mechanical properties of the filling material was investigated. The strength change law of the cemented filling material with mechanism granular gangue of particle size ≤10 mm was explored. PO42.5 cement was used as the filling cement. The SEM technique was adopted to analyze the material generated characteristics during hardening process of the filling paste. The characteristic and appearance of products such as ettringite, calcium hydroxide, and gel in the filling material were analyzed. Finally, the law of strength growth and change of paste cementing backfill material at different curing ages were obtained.

2. Materials

2.1. Mechanism Granular Gangue. The gangue material used in the test was taken from Wantian Coal Mine in Liupanshui City, Guizhou Province. To follow the principle of representativeness, during the normal production period of the mine, coal gangue samples are collected at different time intervals to ensure the uniformity of the samples. The test data are taken as the average of three test results. The gangue samples were rinsed with water to remove the mud and processed by a jaw crusher. Finally, they became the mechanism granular gangue with particle size <10 mm. Before test, the gangue was dried and held in plastic buckets. The physical performance indexes of the mechanism granular gangue are shown in Table 1.

Table 1: Physical performance indexes of mechanism granular gangue.

Specific gravity	Loose bulk density ($kg \cdot m^{-3}$)	Dense bulk density ($kg \cdot m^{-3}$)	Maximum porosity (%)	Minimum porosity (%)	Maximum void ratio	Minimum void ratio	Angle of repose (°)
2.67	1616.98	1780.95	39.438	33.296	0.651	0.499	29.41

Table 2: Physical property indexes of fine sand.

Specific gravity	Loose bulk density ($kg \cdot m^{-3}$)	Dense bulk density ($kg \cdot m^{-3}$)	Maximum porosity (%)	Minimum porosity (%)	Maximum void ratio	Minimum void ratio	Angle of repose (°)
2.61	1506.9	1665.09	42.299	36.207	0.733	0.567	35.51

Table 3: Physical properties indexes of cement.

Specific gravity	Loose bulk density ($kg \cdot m^{-3}$)	Dense bulk density ($kg \cdot m^{-3}$)	Maximum porosity (%)	Minimum porosity (%)	Maximum void ratio	Minimum void ratio	Angle of repose (°)
3.09	980.5	1775.3	68.269	42.546	2.151	0.741	33.57

Table 4: The performance indexes of the test tap water.

Specific gravity	Bulk density ($kg \cdot m^{-3}$)	Chroma (°)	pH	Oxygen consumption ($mg\ L^{-1}$)	NH_3–N ($mg\ L^{-1}$)	ClO_2 extra ($mg\ L^{-1}$)
1.0	1000.0	1	7.12	1.46	0.04	0.21

2.2. Fine Sand. After the fine sand is collected, it is dried it in the air and placed it in a dedicated container. The test data are taken as the average of three test results. The fine river sand used in the test was taken from the traditional building materials. Table 2 shows the physical property indexes of the fine sand.

2.3. Cement. Samples were taken from newly produced bagged cement to avoid moisture affecting the test results. The average of three test results was taken for the test data. The cementitious material used in the test is 42.5 ordinary Portland cement of Qizi Bridge. Table 3 shows the physical property indexes of the cement.

2.4. Water. The mixing water used in the test was ordinary tap water in the laboratory, obtained from Xiangtan Xiangjiang Water Company. Table 4 shows the performance indexes of the tap water.

3. Filling Materials Specimen

3.1. Proportion of Filling Slurry. The mix proportion of filling slurry is selected based on the results of the slump test and the technical conditions of the mine site production; after analysis and discussion of fluidity and mechanical properties, the aggregate (mechanism granular and find sand) cement ratio (α) is 3.5 : 1. The gangue–sand ratio (β) is 3 : 7, 5 : 5, and 7 : 3. According to the liquidity of the paste-filling slurry, the mass fraction (ω) of the paste-filling slurry is 82%, 84%, and 86%, respectively [31]. The specific gravity was measured, and the dosage of every component was determined. The material consumption of mechanism granular gangue, fine sand, cement, and water in the unit volume of filling material is shown in Table 5.

3.2. Preparation of Filling Materials Specimen. The 7.07 cm^3 triplex polymer composite mold was used. The hole in the mold's bottom was sealed to prevent the paste from flowing out when pouring the paste-filling slurry into the mold. Water, cement, mechanism granular gangue, and fine sand were poured into the mixer and mixed for 9 min to form a uniform filling slurry, which was then poured into the mold. During the pouring process, a metal rod was used to tap the edge of the mold and continuously vibrate the filling slurry so that the air bubbles trapped in the filling slurry inside the mold could be discharged and become dense enough. Finally, the mold was placed on the vibrating table for compaction, and then a spatula was used to smooth the top surface of the filling specimen. After casting, the mold would be in the maintenance room for maintenance. After 24 hr, the specimen will be demolded by using the portable air compressor. It is worth noting that the integrity of the specimen should be ensured in the demolding process. The making and demolding process should be strictly followed by the operating instruction.

Table 5: Consumption per unit volume of filling material.

Group number	Mass fraction (ω) (%)	Aggregate cement ratio (α)	Gangue–sand ratio (β)	Material consumption per unit volume ($kg{\cdot}m^{-3}$)			
				Coal gangue	Fine sand	Cement	Water
Group 1	86	3.5 : 1	3 : 7	440	1,026	419	307
	84			418	975	398	341
	82			397	927	378	374
Group 2	86	3.5 : 1	5 : 5	735	735	420	308
	84			698	698	399	342
	82			664	664	379	375
Group 3	86	3.5 : 1	7 : 3	1,031	442	421	308
	84			980	420	400	343
	82			931	399	380	375

4. Performance Test and Analysis of Granular Gangue Fine Sand-Filling Material

The uniaxial compressive strength was measured by a computer program-controlled instrument in the laboratory. Each group of filled material specimens was moistened and maintained at room temperature. The test maintenance ages t were 2, 3, 4, 5, 6, 7, 8, 9, and 10 days, respectively. Nine different groups of material proportion tests were conducted.

4.1. Results and Analysis of Uniaxial Compressive Strength Test

4.1.1. Influence of Gangue–Sand Ratio (β) on Compressive Strength of Filling Specimen. In the case of the same mass fraction (ω) and sand–cement ratio (α) of 3.5 : 1, the uniaxial compressive strength of filling specimen with different gangue–sand ratios (β) is shown in Figure 1. From the overall trend of the graph, when the mass fraction (ω) is 86% or 82% (Figures 1(a) and (b)), with the increase of gangue–sand ratio (β), the specimen solidification speed presents the trend of first increase and then slow down. The strength of the specimen also increases first and then decreases with the age. The effect of gangue–sand ratio (β) on the strength of the specimen is relatively obvious. The uniaxial compressive strength is the largest when gangue–sand ratio (β) is 5 : 5. The strength of the specimen with a gangue ratio (β) of 7 : 3 is the lowest among the three groups. When the curing age is 10 days, the mass fraction (ω) is 86% and 82%, and their strength with the gangue–sand ratio (β) of 5 : 5 is 1.38 times and 1.21 times as strong as that of gangue–sand ratio (β) of 7 : 3, respectively.

When the mass fraction (ω) is 84%, and the sand–cement ratio (α) is 3.5 : 1 (Figure 1(c)), the larger the gangue–sand ratio (β), the slower the setting speed of the specimens and the lower the strength of the specimens at all ages. As shown in Figure 1, when the gangue–sand ratio (β) is 3 : 7, its strength is the largest. The strength begins to decrease slowly at the gangue–sand ratio (β) of 5 : 5. There is a clear downward trend at the gangue–sand ratio (β) of 7 : 3 compared with the gangue–sand ratio (β) of 3 : 7. The strength of the paste-cemented filling material specimen with the 3 : 7 gangue ratio (β) is 1.23–1.61 times as strong as that of the 7 : 3 gangue ratio (β).

4.1.2. Effect of Curing Age on Compressive Strength of Filling Specimen. The uniaxial compressive strength of specimens from 2 to 10 days was compared and analyzed. The strength data of specimens with different mix proportion at each age were expressed graphically using statistical software. The variation curves were obtained, as shown in Figure 2, which were linearly fitted by the origin software, and the relevant results were shown in Table 6. The function between compressive strength and curing age can be described by Equation (1).

$$\sigma = kt, \tag{1}$$

where σ is the uniaxial compressive strength of specimen, t is the curing age of the specimen, and the coefficient k is related to the paste-cemented filling material. Therefore, in the actual project, the fitting formula can be referred to as prediction of the uniaxial compressive strength of filling body of the mechanism granular gangue and fine sand.

As shown in Figure 2, the specimens' uniaxial compressive strength gradually increases with the curing age. In general, the curve of the compressive strength with curing age shows an increasing progressive trend and finally reaches a higher value at the 10th curing age. From the overall trend of the dotted line graph, the compressive strength of the specimens will continue to increase in the coming period. For the specimens with the paste mass fraction (ω) of 86% (Figure 2(a)), when gangue–sand ratios (β) is 3 : 7, 5 : 5, and 7 : 3, the compressive strengths are, respectively, 3.164, 2.617, and 1.882 MPa at 3 days, 6.152, 5.725, and 7.312 MPa at 7 days, and 8.962, 11.031, and 8.011 MPa at 10 days. It can be seen that the specimens has faster strength growth in the early stage.

From the practical point of view, the early strength of filling body is very important for the environment and engineering needs. The performance of the above paste-cemented filling material with a paste mass fraction (ω) of 86% and gangue–sand ratio (β) of 3 :7, 5 : 5, and 7 : 3 can meet the practical requirements. For the specimens with a paste mass fraction (ω) of 82% and gangue–sand ratios (β) of 3 : 7, 5 : 5,

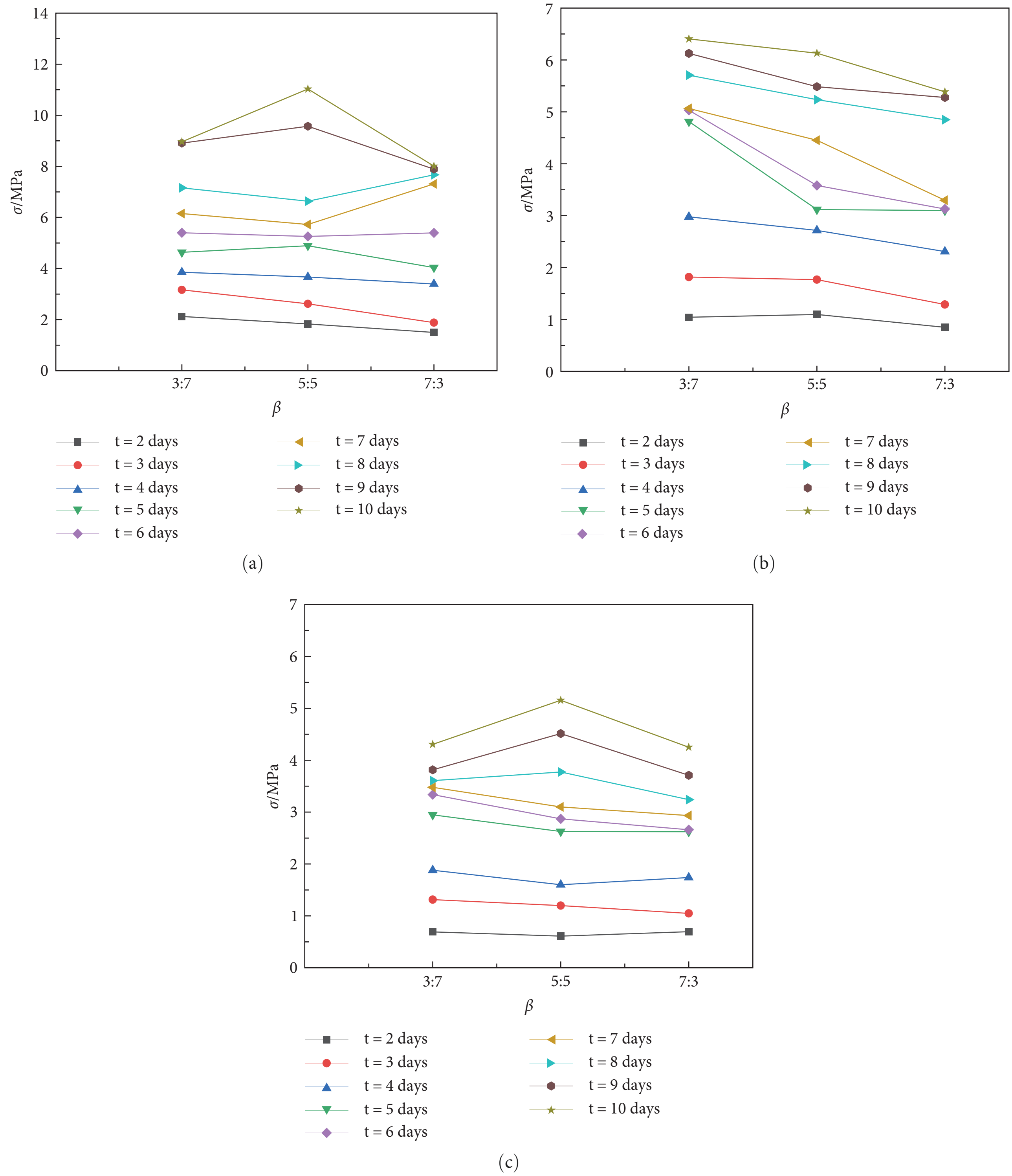

Figure 1: Uniaxial compressive strength of specimens under different gangue–sand ratio (β). (a) $\omega = 86\%$; (b) $\omega = 84\%$; (c) $\omega = 82\%$.

and 7 : 3, the strengths are, respectively, 1.314, 3.479, and 1.199 MPa at 3 days and 3.1, 1.047, and 2.934 MPa at 7 days. Compared with uniaxial compressive strength at 3 days, they, respectively, increased by 2.651, 2.591, and 2.802 times. The uniaxial compressive strengths of the above three groups are, respectively, 4.307, 5.155, and 4.251 MPa at 10 days.

4.1.3. Effect of Mass Fraction (ω) on the Compressive Strength of Filling Specimen. As shown in Figure 3, for the filling material specimens with same sand–cement ratio (α) of 3.5 : 1, their strength positively relates to the mass fraction (ω). As the strength of specimens at 2, 3, 7, and 10 days curing ages, the strength of the paste-cemented filling material has an obvious growth with the increase of the mass fraction (ω). The uniaxial

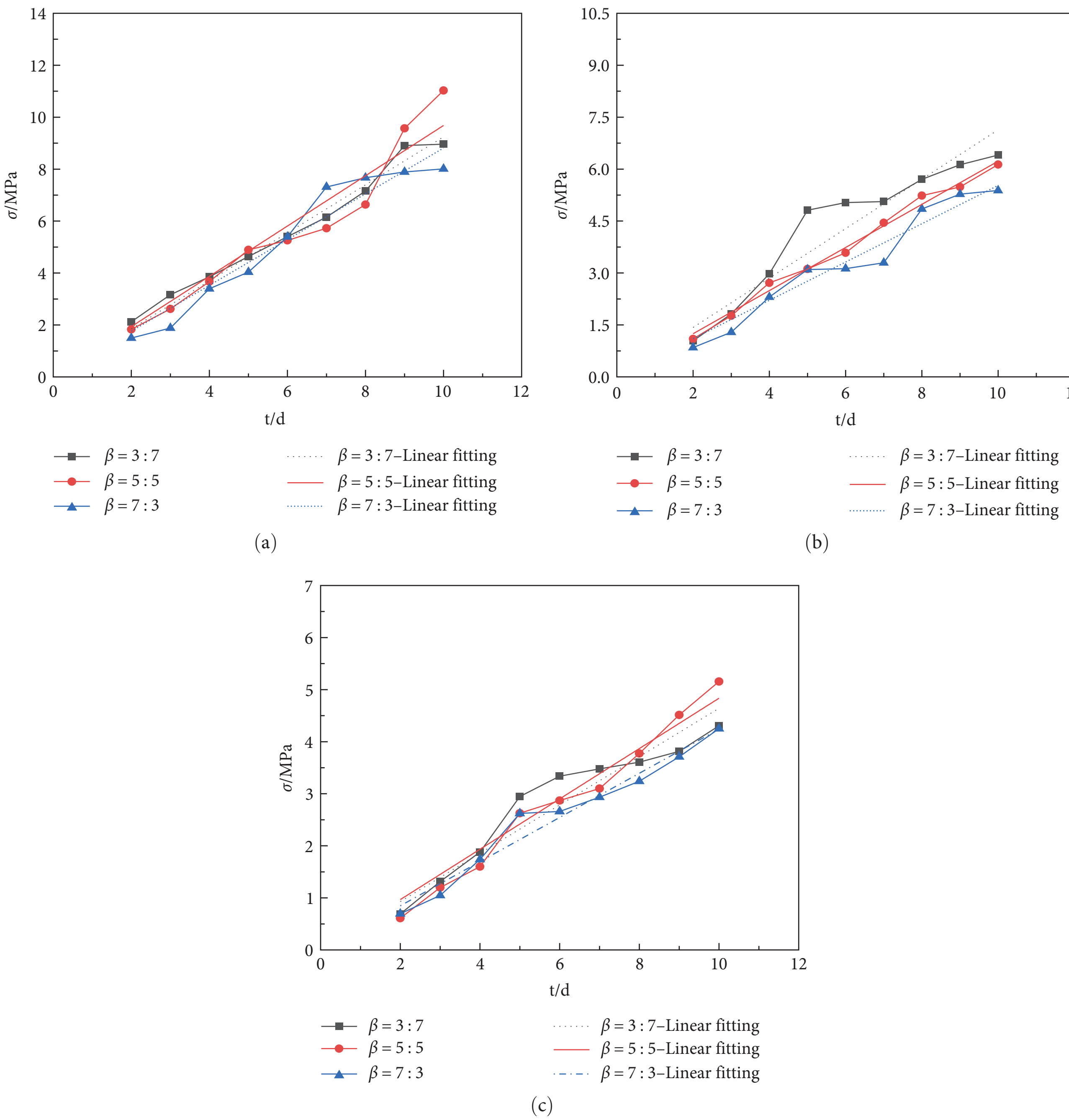

Figure 2: Uniaxial compressive strength of specimens at different curing ages. (a) $\omega = 86\%$; (b) $\omega = 84\%$; (c) $\omega = 82\%$.

Table 6: Parameter values and correlation coefficients of each fitting function.

Group number	Specimen number	k	R^2
Group 1	1	0.92411	0.99706
	2	0.96822	0.98359
	3	0.88138	0.98824
Group 2	4	0.71350	0.98294
	5	0.62278	0.99846
	6	0.55200	0.99066
Group 3	7	0.46409	0.98567
	8	0.48349	0.99297
	9	0.42420	0.99387

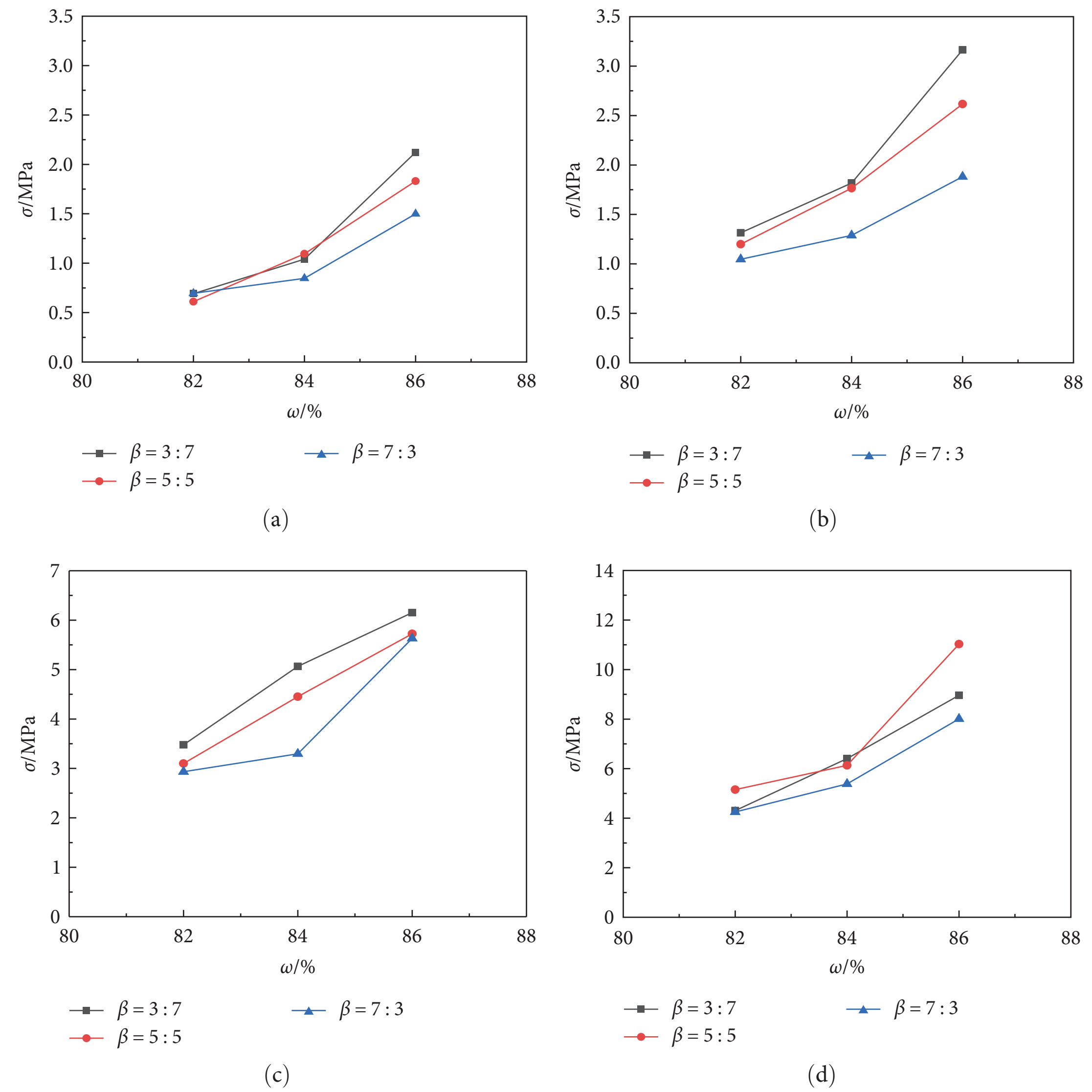

Figure 3: Uniaxial compressive strength of specimens with different mass fractions (ω) of filling materials. (a) $t = 2$ days; (b) $t = 3$ days; (c) $t = 7$ days; (d) $t = 10$ days.

compressive strength of the filling material specimens increases continuously as the mass fraction (ω) increases. When the gangue–sand ratio (β) and sand–cement ratio (α) are constants, the larger the mass fraction, the higher the uniaxial compressive strength. The statistical software was used for comparative analysis. When the curing age is the same, with the increase of the mass fraction (ω), there is also a specific difference in the strength growth law of different gangue–sand ratio (β). From the overall view of the change curve, as shown in Figure 3, with the increasing mass fraction (ω), the strength of filling material with the gangue–sand ratio (β) of 3 : 7 increases the most, and the strength increases the least when the gangue–sand ratio (β) is 7 : 3.

4.2. Hydration Mechanism of Cementitious Materials. The cementitious material used in the test is PO42.5 grade ordinary Portland cement with good versatility on the market today. Some researchers have developed new cementitious materials. They have achieved good results in serving costs and safety technologies in filling cementitious materials. They developed new cementitious materials for low-cost mine filling that reflect better the cost performance compared with PO42.5 ordinary Portland cement [32, 33]. This test aims to ensure that it does not reduce the strength of the paste cementing-filling material, to reduce the cost of mine filling further, and to solve the problem of bulk better solid waste emissions. Future research can start the development of different types of new filling cementitious materials to achieve the purpose of energy saving, emission reduction and cost reduction, and efficiency increase.

During the filling process, the physical and chemical properties of mechanism granular gangue and fine sand will not change. However, the physical and chemical properties of the cementitious material will change. Aggregates are cemented together to form a whole with a particular strength. In order to analyze the hydration reaction process

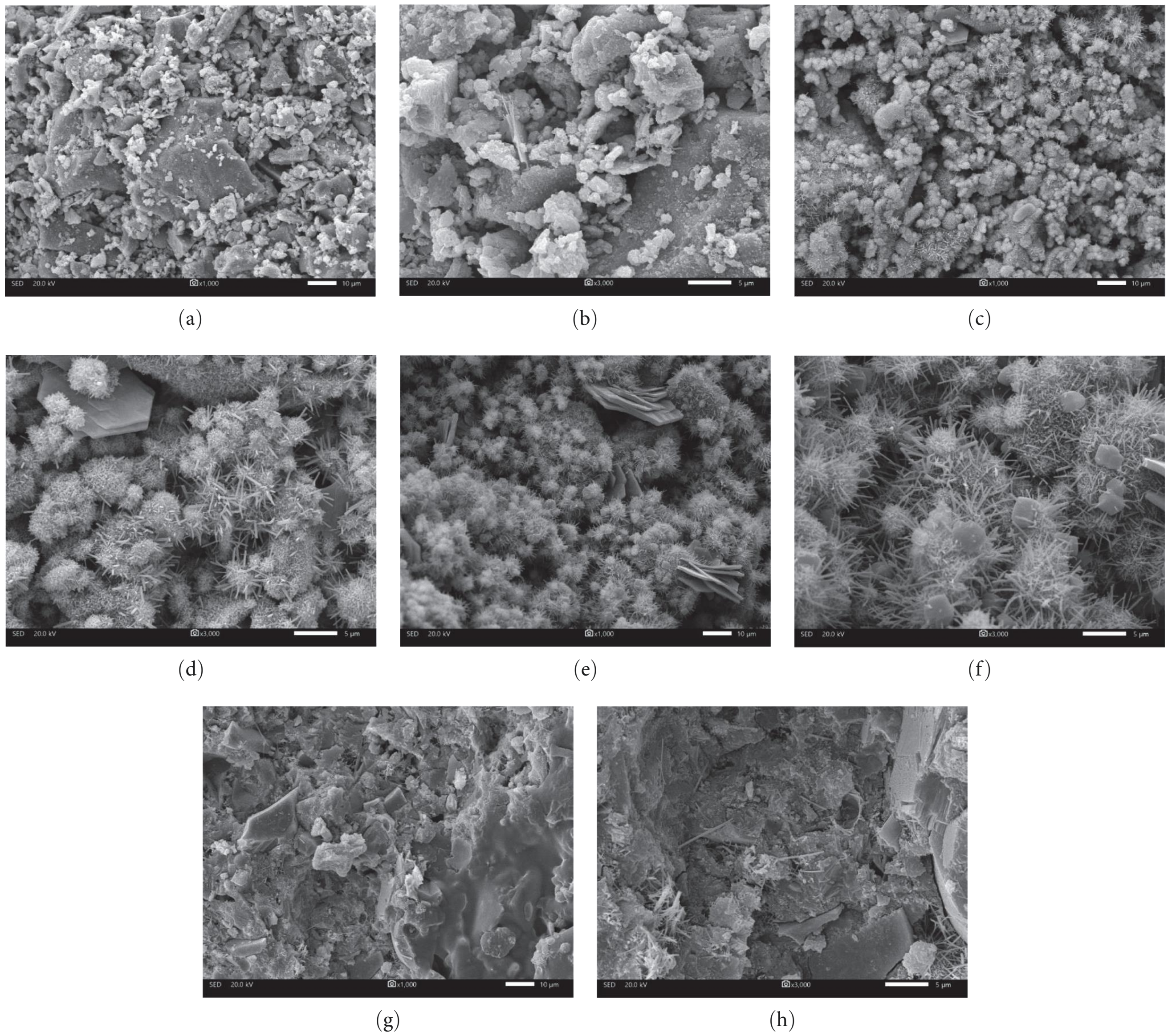

Figure 4: SEM microstructure of PO42.5 grade cement net paste at different curing ages. (a) $t = 1$ day (1,000 times); (b) $t = 1$ day (3,000 times); (c) $t = 3$ days (1,000 times); (d) $t = 3$ days (3,000 times); (e) $t = 7$ days (1,000 times); (f) $t = 7$ days (3,000 times); (g) $t = 10$ days (1,000 times); (h) $t = 10$ days (3,000 times).

of cement, the SEM technique was used to analyze the morphology characteristics of hydration products to analyze the mechanism of strength growth. Figure 4 shows the SEM microstructure of cement paste under different curing ages.

(1) As shown in Figure 4(a), the hydration product of the cement paste with a curing age of 1 day is mainly calcium hydroxide with a flaky structure. In addition, a few needle-like ettringite crystals appear. The flaky calcium hydroxide in the filling material causes many holes. As a result, the overall structure of filling material becomes sparse and loose. Hence, the filling material only has low strength with a curing age of 1 day.

(2) As shown in Figure 4(b), it can be seen that the content of calcium hydroxide increases. In addition, the C–S–H gel starts to appear in small amounts on the surface of coarse and fine aggregates. A large number of voids can still be seen in the material. The strength increased at the curing age of 3 days.

(3) As the curing age reaches 7 days, the amorphous C–S–H gel gradually grows and intertwines the aggregate with the hydration products, making the structure more compact than at 3 days curing age.

(4) As shown in Figure 4(d), the C–S–H gel, calcium hydroxide crystals, and needle-like calcium alumina crystals formed at this time are interlaced and filled in the voids of the slurry, which make the aggregate

and hydration products connect into a close piece and interweave to form a dense internal structure, and the compressive strength of the material is higher.

5. Conclusions

To reduce the potential geological hazards in the coal mine goaf and to improve the utilization rate of coal gangue resource to solve the problem of safe discharge of bulk industrial solid waste, the paper was conduct the study of filling materials. To obtain the optimal mix proportion, the flow performance and mechanical property of filling material with different gangue–sand ratio and mass fraction at different curing age were investigated. The main conclusions are listed as follows:

(1) The sand–cement ratio (α), gangue–sand ratio (β), and a mass fraction (ω) are essential factors affecting the mechanical properties of cementitious filling materials. The compactness of the block with more cement is better than that of less cement, so its strength is larger. When the proportion of cement in the filling slurry is unchanged, increasing the mass fraction of filling slurry is an excellent way to improve the strength of the filling material.

(2) The condensation and hardening performance of the filling specimens with different ratios of the nine groups are normal. The mold can be demolded typically 24 hr after the completion of its pouring. Moreover, the surface of the specimen after the mold release is slightly concave and convex. Several groups of paste-filling paste analyzed in this experiment are all high in mass fraction (ω), and their consolidation and contraction speed are relatively fast, thus shortening the coagulation hardening process of paste-filling slurry to a certain extent.

(3) According to the analysis of the flow ability of the paste-filling slurry and the uniaxial compressive test of filling body, it can be seen that other conditions are the same, the fluidity of the paste-filling slurry with gangue-sand ratio (β) of 5 : 5 is better than the fluidity of the two groups of gangue–sand ratio (β) of 3 : 7 and 7 : 3. Moreover, their compressive strength is close. Therefore, the filling material with a gangue ratio (β) of 5 : 5 is the appropriate.

(4) According to the linear fitting results of compressive strength and curing age, the correlation coefficient R^2 is between 0.99143 and 0.99923. So, it can predict the compressive strength of filling body by Equation (1).

(5) Through the SEM electron microscopy test of cement slurry, the hydration products and microstructure of each stage of paste-filling slurry are almost the same to the ordinary Portland cement. The mechanism of granular coal gangue and fine sand as inert materials does not affect the hydration reaction of the cement.

Data Availability

The data that support the findings of this study are available from the corresponding author.

Conflicts of Interest

The authors declare that they have no conflicts of interest.

Authors' Contributions

Daiqiang Deng, Runze Wang, and Guodong Cao wrote the main text of the manuscript. Yihua Liang, Jinkuan Fan, Yunfan Ma, and Yu Gao collected and analyzed the data. All authors reviewed and commented on the manuscript.

Acknowledgments

This work was supported by the NSFC Projects of China (51764009), the Provincial Natural Science Foundation of Hunan (2023JJ50041), the Doctoral Research Project of Xiangtan University (22QDZ28, 22QDZ35), the Guizhou Institute of Technology High-level Talent Research Start-up Funding Project—Research on Optimization of Particle grading of Modified filling Materials (Project Approval Number/Contract Number XJGC20190652). The authors are grateful for the financial support for this research.

References

[1] X. Daguang, "Research status of coal combustion technology in the United States-report on visit to the United States," *Power System Engineering*, vol. 59, no. 4, pp. 1–10, 1988.

[2] Z. Guanghua, "Energy pollution in Japan and its control policies," *World Environment*, vol. 23, no. 2, pp. 11–13, 1986.

[3] X. Futian, "Power industry in Spain," *Shandong Electric Power*, vol. 32, no. 4, pp. 97–100, 1994.

[4] M. Hendryx, N. Higginbotham, B. Ewald, and L. H. Connor, "Air quality in association with rural coal mining and combustion in New South Wales Australia: air quality in rural Australia," *The Journal of Rural Health*, vol. 35, no. 4, pp. 27–527, 2018.

[5] L. Qian, "Australia will lead the energy transition," *Oil–Gas Field Surface Engineering*, vol. 39, no. 10, Article ID 7, 2020.

[6] L. Zhongdong, "The year of light in the Netherlands, Toyota in Japan, and Sono in Germany," *Light Vehicles*, vol. 25, no. 7, pp. 64–69, 2020.

[7] J. Lambertz, "Efficient power generation in coal- and gas-fired power plants," *VGB PowerTech*, vol. 1, no. 2, Article ID 85, 2005.

[8] L. Jun, "Research on regulated asset base (RAB) model for nuclear power in the UK," *Sino-Global Energy*, vol. 26, no. 1, pp. 22–27, 2021.

[9] T. Yishui, S. Ming, K. Geng, M. Linwei, and S. Si, "Development strategy of biomass economy in China," *Chinese Journal of Engineering Science*, vol. 23, no. 1, pp. 133–140, 2021.

[10] W. Huang, J. Han, Y. Wsang, Y. Shen, and L. Chen, "Strategies and countermeasures for ensuring energy security in China," *Chinese Journal of Engineering Science*, vol. 23, no. 1, pp. 112–117, 2021.

[11] Y.-Z. Zhang, "Study on the path of, near-zero emission, coal-based clean energy ecosystem development," *Frontiers of Engineering Management*, vol. 1, no. 1, pp. 37–41, 2014.

[12] J. He, C. Fu, and Y. Long, "Promoting the high-quality development of central China through energy revolution: theoretic analysis and implementation paths," *Chinese Journal of Engineering Science*, vol. 23, no. 1, pp. 60–67, 2021.

[13] T. F. Tomb, A. J. Gero, and J. Kogut, "Analysis of quartz exposure data obtained from underground and surface coal mining operations," *Applied Occupational and Environmental Hygiene*, vol. 10, no. 12, pp. 1019–1026, 1995.

[14] C. Xie, H. Nguyen, X.-N. Bui, V.-T. Nguyen, and J. Zhou, "Predicting roof displacement of roadways in underground coal mines using adaptive neuro-fuzzy inference system optimized by various physics-based optimization algorithms," *Journal of Rock Mechanics and Geotechnical Engineering*, vol. 13, no. 6, pp. 1452–1465, 2021.

[15] D. Ma, H. Duan, J. Zhang, X. Liu, and Z. Li, "Numerical simulation of water–silt inrush hazard of fault rock: a three-phase flow model," *Rock Mechanics and Rock Engineering*, vol. 55, no. 8, pp. 5163–5182, 2022.

[16] A. K. Goodwin, M. A. O'Neill, and W. F. Anderson, "The use of X-ray computer tomography to investigate particulate interactions within opencast coal mine backfills," *Engineering Geology*, vol. 70, no. 3-4, pp. 331–341, 2003.

[17] M. Li, J. Zhang, W. Song, and D. M. Germain, "Recycling of crushed waste rock as backfilling material in coal mine: effects of particle size on compaction behaviors," *Environmental Science and Pollution Research International*, vol. 26, no. 9, pp. 78–8797, 2019.

[18] D. Ma, H. Duan, and J. Zhang, "Solid grain migration on hydraulic properties of fault rocks in underground mining tunnel: radial seepage experiments and verification of permeability prediction," *Tunnelling and Underground Space Technology*, vol. 126, Article ID 104525, 2022.

[19] Q. Sun, J. Zhang, and N. Zhou, "Roadway backfill coal mining to preserve surface water in Western China," *Mine Water and the Environment*, vol. 37, no. 2, pp. 366–375, 2018.

[20] W. Lv, Y. Wu, L. Ming, and J. Yin, "Migration law of the roof of a composited backfilling longwall face in a steeply dipping coal seam," *Minerals*, vol. 9, no. 3, pp. 188–249, 2019.

[21] H. Yanli, W. Wenfeng, and B. Zhengfu, "Prospects of resource utilization and disposal of coal-based solid wastes in Xinjiang," *Coal Science and Technology*, vol. 49, no. 1, pp. 319–330, 2021.

[22] G. Meng, M. Li, Z. Wu, H. Ma, and Y. Wang, "The effects of high temperature on the compaction behavior of waste rock backfill materials in deep coal mines," *Bulletin of Engineering Geology and the Environment*, vol. 79, no. 2, pp. 845–855, 2020.

[23] Z. Wang, J. Zhang, M. Li, S. Guo, J. Zhang, and G. Zhu, "Experimental study of microorganism-induced calcium carbonate precipitation to solidify coal gangue as backfill materials: mechanical properties and microstructure," *Environmental Science and Pollution Research International*, vol. 29, no. 30, pp. 45774–45782, 2022.

[24] J. Jin, Z. Qin, X. Lü et al., "Rheology control of self-consolidating cement-tailings grout for the feasible use in coal gangue-filled backfill," *Construction and Building Materials*, vol. 316, Article ID 125836, 2022.

[25] X. Deng, Z. Yuan, Y. Li, H. Liu, J. Feng, and B. de Wit, "Experimental study on the mechanical properties of microbial mixed backfill," *Construction and Building Materials*, vol. 265, Article ID 120643, 2020.

[26] I. Cavusoglu, E. Yilmaz, and A. O. Yilmaz, "Additivity effect on properties of cemented coal fly ash backfill containing water-reducing admixtures," *Construction and Building Materials*, vol. 267, Article ID 121021, 2020.

[27] X. Deng, J. Zhang, B. Klein, B. de Wit, and J. Zhang, "Time-dependent lateral pressure of the filling barricade for roadway cemented backfill mining technology," *Mechanics of Time-Dependent Materials*, vol. 24, no. 1, pp. 41–58, 2020.

[28] C. Chen, H. Yang, and Z. Fan, "Research on the influence of machine-made sand type on the workability and mechanical properties of mortar," *Building Structure*, vol. 51, no. S2, pp. 1020–1025, 2021.

[29] S. O. Ekolu, F. Solomon, and A. Naghizadeh, "Abandoned mine tailings and coal ash industrial wastes for sustainable production of geopolymer brick masonry: South African case study," *Key Engineering Materials*, vol. 916, no. 23, pp. 130–135, 2022.

[30] A. Bauerek, J. Diatta, Ł. Pierzchała, A. Więckol-Ryk, and A. Krzemień, "Development of soil substitutes for the sustainable land reclamation of coal mine-affected areas," *Sustainability*, vol. 14, no. 8, pp. 4604–4604, 2022.

[31] D. Deng, J. Fan, G. Cao et al., "Study on sound propagation performance of mechanized coal gangue-fine sand filling body," *Shock and Vibration*, vol. 2023, Article ID 4904326, 10 pages, 2023.

[32] A. Khayrutdinov, I. Paleev, and S. Artemov, "Replacement of traditional components of the backfill mixture with man-made waste," *IOP Conference Series: Earth and Environmental Science*, vol. 942, no. 1, Article ID 012005, 2021.

[33] C. N. Ghosh, S. Behera, D. P. Mishra, P. Singh, and J. Buragohain, "Strength development and microstructural investigation of lead-zinc mill tailings based paste backfill with fly ash as alternative binder," *Cement and Concrete Composites pp.*, vol. 109, Article ID 103553, 2020.